Available online at https://jcst.rsu.ac.th
Formerly Rangsit Journal of Arts and Sciences (RJAS)

Journal of Current Science and Technology, July-December 2019 JCST Vol. 9 No. 2, pp. 77-87

ISSN 2630-0583 (Print)/ISSN 2630-0656 (Online)

Concerted hydrogen bond and Hirshfeld surface analysis of Curcumin, *Curcuma longa*

Saifon A. Kohnhorst[1*] and Saowanit Saithong[2]

[1]Chemistry Program, Faculty of Science and Technology, Nakhon Ratchasima Rajabhat University, Nakhon Ratchasima 30000, Thailand
[2]Department of Chemistry and Center of Excellence for Innovation in Chemistry, Faculty of Science, Prince of Songkla University, Hat Yai, Songkhla 90112, Thailand

*Corresponding author; E-mail: saifon.k@nrru.ac.th

Received 18 August 2019; Revised 30 October 2019; Accepted 20 November 2019
Published online 21 December 2019

Abstract

Curcumin ($C_{21}H_{20}O_6$) crystals were obtained from attempts to cocrystallize curcumin with amino acid in mixed ethanol/methanol solvent. The curcumin structure, solved and refined by single crystal X-ray diffraction, exists in the enol form. Analysis of the electron density demonstrates nonstatistical disorder of the positions for the enol proton forming a strong hydrogen bond stabilizing the enol form within the curcumin molecule. Analysis of the intermolecular packing of the molecules shows that the crystal structure is assembled via two strong supramolecular O–H···O interactions with distances of 2.4696(19) - 3.028(2) Å and a weak C–H···O hydrogen bond, distance of 4.046(3) Å. The hydrogen bond graph set notation was assigned $R_6^2(36)$ pattern. Hirshfeld surface analysis indicates that the curcumin crystal structure is stabilized by the weak hydrogen bonds. Crystal Data: $C_{21}H_{20}O_6$ (M_r = 368.37 Daltons: monoclinic, space group $P2/n$ (No. 13), a = 12.6956(3) Å, b = 7.2093(2) Å, c = 19.9362(5) Å, β = 95.276(2)°, V = 1816.96(8) Å^3, Z = 4.

Keywords**:** *crystal structure, curcuma longa, curcumin, curcuminoid, Hirshfeld surface analysis, hydrogen bond*

1. Introduction

Crystal engineering (Desiraju, 2018) is a design of new solids with desired physical and chemical properties which plays an important role in supramolecular chemistry (Nangia & Desiraju, 2018). Applications in drug-receptor interactions and drug design, in chemical and biological processes including molecular recognition, protein stability, carbohydrate crystals, and in the bioactivity of macromolecules (Jeffrey & Saenger, 1991). Many pharmaceutical compounds include functional groups capable of participating in hydrogen-bonding interactions; therefore, materials capable of acting as hydrogen-bond receptors are of considerable concern for these applications (Hutchins, 2018). Cocrystallization has been shown to improve drug properties such as solubility and bioavailability of class II and IV drugs (Chavda, Patel, & Anand, 2010).

Curcumin, a hydrophobic natural product compound having the chemical name of 1,7-bis(4-hydroxy-3-methoxyphenyl)-1,6-heptadiene-3,5-dione, was extracted from turmeric, *Curcuma longa* (Matlinska et al., 2018). Curcumin is widely used as a food additive as a coloring agent and spice. It has a wide variety of medicinal benefits, such as anticancer, anti-inflammatory, anti-HIV, antimalarial, and antioxidant properties (Skieneh, Sathisaran, Dalvi, & Rohani, 2017). Curcumin belongs to the group of β-diketones and exhibits tautomerism between enol and keto structures (Sathisaran & Dalvi, 2017), as shown in Figure 1.

Consistent with the importance of curcumin, its crystal structure has been studied and reported multiple times. The first determination (polymorph I) was reported by Tonnessen, Karlsen, and Mostad (1982). Crystalline polymorphs II and III were investigated and reported by Sanphui, Goud, Khandavilli, Bhanoth and Nangia (2011). Redeterminations of the single crystal X-ray structure of polymorph I has also been reported (Ishigami, Goto, Masuda, & Suzuki, 1999; Parimita, Ramshankar, Suresh, & Guru Row, 2007). There is inconsistency in the modeling of the enolizable proton in polymorph I in the three previous reports, as well as inconsistency of the structural parameters and the electron density maps in the third report. Thus, another redetermination of the structure of

polymorph I of curcumin is merited and reported herein.

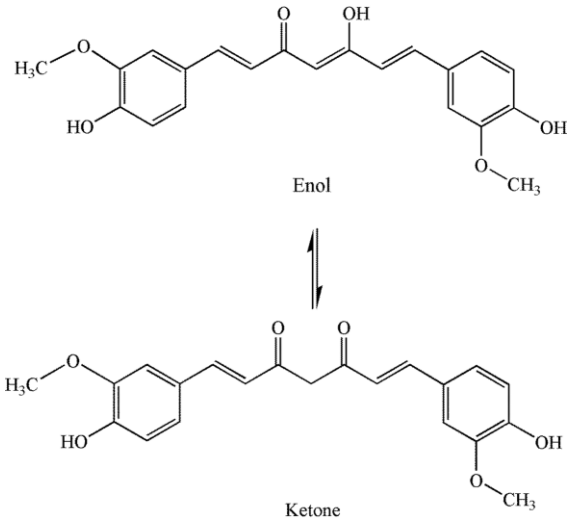

Figure 1 Molecular structure of two forms of curcumin

2. Objectives

Curcumin is an essential herb that can be consumed for treatment of several conditions such as cancer, arthritis, pain, bruises, gastrointestinal diarrhea, swelling, and much more. Curcumin is a low solubility and thus a low bioavailability material that challenges scientists to improve curcumin as a cocrystal remediation application. This research aims to understand the supramolecular interactions in the crystal structure of curcumin.

3. Materials and methods

3.1 Experimental preparation

Attempts to cocrystallize curcumin with amino acids by the grinding method and by a liquid-liquid technique (dissolving the components in 10 mL of ethanol and adding a 1 mL layer of methanol on top of the solution and keeping in the dark at room temperature for one month). The crystals were collected after four weeks by filtering the clear yellow crystals and leaving them to air-dry at room temperature.

3.2 X-ray crystal structure determination and refinement

A suitable single crystal was selected and the crystal was mounted on a mylar loop with grease, then measured on a SuperNova, single source at offset/far, HyPix3000 diffractometer. The crystal was kept at 295 K during data collection. Structure solution and refinements were analyzed using *OLEX2* (Dolomanov, Bourhis, Gildea, Howard, & Puschmann, 2009), *ShelXle* (Hubschle, Sheldrick, & Dittrich, 2011), the structure was solved by *SHELXT* (Sheldrick, 2015a) structure solution program using intrinsic phasing and refined with the *SHELXL* (Sheldrick, 2015b) refinement package using least-squares minimization. Crystallographic illustrations were drawn using *ORTEP3* (Farrugia, 2012).

Solution and preliminary refinement, including location of positions for all unique H atoms, was entirely routine. All H atoms except that between O3 and O4 were included in the model in chemically sensible geometrically idealized positions with default distances assigned by the *SHELXL* program (d[C–$H_{methylene}$] = 0.93 Å, d[C–H_{methyl}] = 0.96 Å, d[O–$H_{hydroxy}$] = 0.82 Å) as riding-atom contributors with the added provision that the methyl and hydroxy H atoms were allowed to rotate about the vector from the attached atom to

adjacent C atom. Non-H atoms refined with anisotropic atomic displacement parameters, and H atoms given isotropic atomic displacement parameters of U[$H_{methylene}$] = 1.2U_{eq}[$C_{attached}$], U[H_{methyl}] = 1.5U_{eq}[$C_{attached}$], and U[$H_{hydroxy}$] = 1.2U_{eq}[$O_{attached}$].

Careful examination of electron density difference maps of the region between O3 and O4 before inclusion of H3O4 revealed an extension of electron density in the region where idealized H-atom positions would be placed in the event that there was a disordered enol form in the crystal structure with a slight preponderance of electron density on the position near O3. A number of models for the position(s) of the enolized H atom were refined. The discrepancy index, R_1 ranged from 0.0512 to 0.0517. Models **E**, **F**, **G,** and **H** had similar, and the lowest values for wR_2 at 0.1575 – 0.1576 indicating that their common features constitute the best model from the room temperature X-ray data in this report.

Models **A** – **C** assume a single H-atom position between O3 and O4, *i.e.* the resonance stabilized hydrogen bond model. Model **A**, a single fully occupied refined H3O4 position equidistant from O3 and O4 with a refined isotropic U[H3O4] (result, d[O3–H3O4] = d[O4–H3O4] = 1.25 Å, U[H3O4] = 0.157 Å^2); Model **B**, Model **A** plus refined isotropic U[H] for all H atoms (result, U[$H_{methylene}$] in general range of 0.05 to 0.06 Å^2, U[H11] = 0.056 Å^2, U[H3O4] = 0.152 Å^2); Model **C**, a single fully occupied unrestrained refined H3O4 position with refined isotropic U[H3O4] and U[H11] (result, d[O3–H3O4] = 1.19 Å, d[O4–H3O4] = 1.32 Å, U[H11] = 0.055 Å^2, U[H3O4] = 0.156 Å^2).

Models **D** – **H** assume two H-atom positions between O3 and O4, *i.e.* a disordered enol form. Model **D**, two one-half occupancy H3O and H4O positions with H atom positions as riding atom contributors with positions allowed to rotate about the O3–C10 and O4–C12 vectors, respectively, with d[O3-H3O] = d[O4-H4O] = 0.82 Å (*SHELXL* default distance) and with refined isotropic atomic displacement parameters for all H except U[H_{methyl}] = 1.5U_{eq}[$C_{attached}$] and U[H3O] = U[H4O] (result, U[H3O] = U[H4O] = 0.0687 Å^2); Model **E**, two one-half occupancy H3O and H4O positions refined with a restraint that d[O3-H3O] and d[O4-H4O] remain similar, and with a refined isotropic U[H3O] = U[H4O] (result, d[O3–H3O] = 0.759 Å, d[O4–H4O] = 0.755 Å, U[H3O] = U[H4O] = 0.0547 Å^2); Model **F**, similar to Model **E**, except allow the occupancy factor, occ[H3O] to refine with occ[H4O] = (1.00 – occ[H3O]), (result, d[O3–H3O] = 0.76(3) Å, d[O4–H4O] = 0.75(3) Å, occ[H3O] = 0.51(3), U[H3O] = U[H4O] = 0.053(9) Å^2); Model **G**, similar to Model **F**, except remove the restraints on d[O3-H3O] and d[O4-H4O] (result, R_1 = 0.0512, wR_2 at 0.1575, d[O3–H3O] = 0.85(5) Å, d[O4–H4O] = 0.64(6) Å, U[H11] = 0.053 Å^2, U[H3O] = U[H4O] = 0.053(10) Å^2).

Model **H**, (reported model) assume a disordered enol form with two nonequivalent H-atom positions between O3 and O4 with refined occupancy factors constrained to sum to 1.000, and a single isotropic atomic displacement parameter, U[H3O] = U[H4O], for H3O and H4O. Restrain d[O3-H3O] and d[O4-H4O] to remain similar. Refine anisotropic non-H atoms and isotropic atomic displacement parameters for H atoms except U[H_{methyl}] = 1.5U_{eq}[$C_{attached}$]. (result, R_1 = 0.0512, wR_2 = 0.1575, *gof* = 1.087, d[O3–H3O] = 0.759(26) Å, d[O4–H4O] = 0.755(26) Å, occ[H3O] = 0.508(31), U[H11] = 0.056(6) Å^2, U[H3O] = U[H4O] = 0.053(9) Å^2, ρ_{max} = 0.26 e Å^{-3}).

4. Results and discussion

4.1 FTIR structure analysis

The FT-IR vibrational frequencies of the crystalline curcumin product (Figure 2) were observed; the O–H stretching band was assigned near 3500 cm^{-1}, the C=O frequency at 1626 cm^{-1}, the broad band aromatic C=C at 1504 cm^{-1}, phenol C–O at 1427 cm^{-1}, and enol C–O at 1273 cm^{-1}, respectively.

4.2 Crystal structure analysis

Attempts to crystallize curcumin with amino acids were described in the experimental section. The data crystal for the current study was obtained from attempts to crystallize curcumin with amino acids in ethanol at room temperature after four weeks. The crystal data, data collection, and structure refinement parameters are given in Table 1.

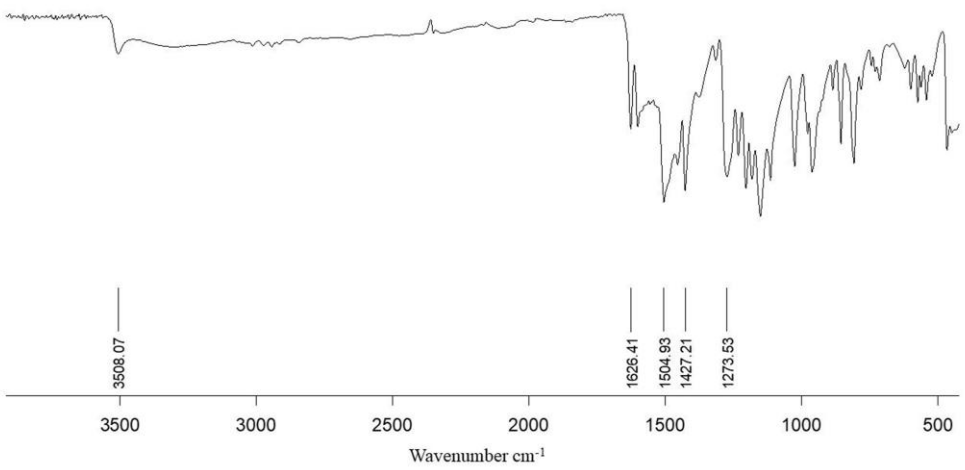

Figure 2 Attenuated total reflection Fourier transform infrared spectra of curcumin

Table 1 Crystal data, data collection, and structure parameters for the present work

Crystal data	
Chemical formula	$C_{21}H_{20}O_6$
M_r (Daltons)	368.37
Crystal system, Space group	Monoclinic, *P*2/n
Temperature (K)	298
a, *b*, *c* (Å)	12.6956(3), 7.2093(2), 19.9362(5)
α, β, γ (°)	90, 95.276(2), 90
V (Å^3)	1816.96(8)
Z	4
D_{calcd} (g cm^{-3})	1.347
Radiation type	Mo $K\alpha$
μ (mm^{-1})	0.099
Data collection	
Diffractometer	Rigaku, HyPix3000
No. of measured, independent and observed [$I > 2\sigma(I)$] reflections	25648, 3956, 2815
R_{int}	0.0418
$(\sin \theta/\lambda)_{max}$ (Å^{-1})	0.65
Refinement	
Refinement on F^2	
$R[F^2 > 2\sigma(F^2)]$, $wR(F^2)$, *S*	0.0512, 0.1575, 1.087
No. of reflections	3956
No. of parameters	270
No. of restraints	2
H-atom treatment	H atoms treated by a mixture of independent and constrained refinement
$\Delta\rho_{max}$, $\Delta\rho_{min}$ (e Å^{-3})	0.26, -0.30

JCST Vol. 9 No. 2 Jul.-Dec. 2019, pp. 77-87
ISSN 2630-0583 (Print)/ISSN 2630-0656 (Online)

The crystal structure of curcumin is shown in Figure 3. Bond lengths and angles are given in supporting information. Individual bond lengths and angles are not significantly different from those of the previous report (Parimita et al., 2007) with the exception of the parameters relating to the enol ring. The molecule is distorted by rotation of −152° about the C8−C9 bond allowing ring A of the molecule to ride above ring B as shown in Figure 4, similar with Matlinska et al. (2018).

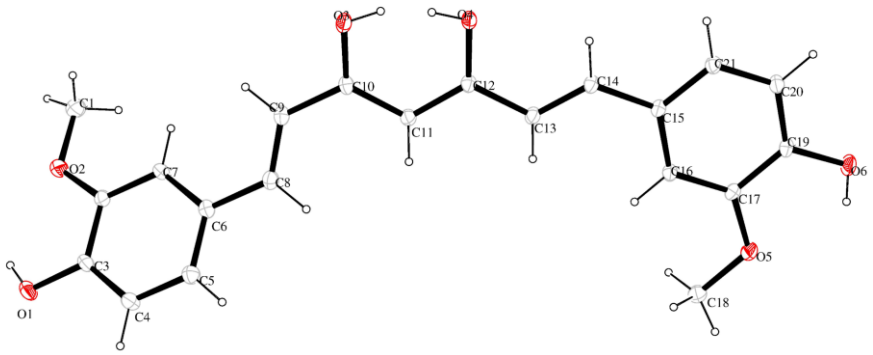

Figure 3 Perspective view of curcumin crystal structure

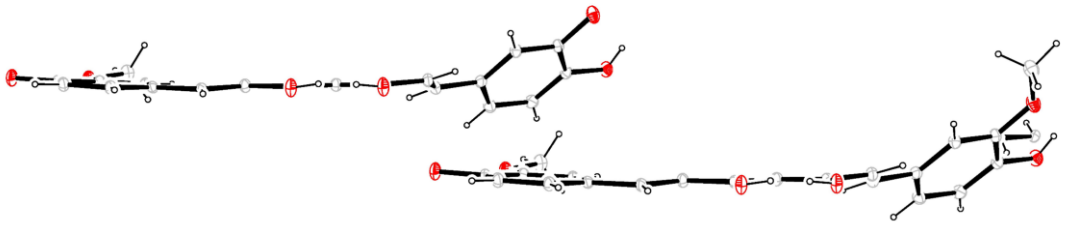

Figure 4 The tilting of the phenol ring in the molecule

Atom labeling of the enol-ring atoms is given in Figure 5, below. The illustrated H-atom positions on atoms O3 and O4 are mutually exclusive; the occ[H3O] = 0.508(31) and occ[H4O] = 1.000 – occ[H3O]. Thermal ellipsoids drawn at 50 % probability level. Hydrogen atoms drawn as arbitrarily small spheres for clarity.

There has been considerable discussion of the nature of the enolizable H atom, including a solid state NMR-quantum chemical theoretical study addressing the proton probability distribution of the curcumin enolizable H atom (Kong et al., 2014). Kong et al. (2014) also evaluated energies of the three relevant localized-proton states (here H3O in Model **H**, H3O4 in Model **C**, and H4O in Model **H**) obtaining the relative energy values, 0, 5.3, and 4.7 kJ mol^{-1}, respectively. Examination of the resonance-assisted hydrogen bond parameters in the previous structure report of Parimita et al. (2007) suggests a model deficiency. The report states that the enol H atom is symmetrically positioned and has full occupancy in the crystal structure. However, the supporting documentation shows that the refined isotropic atomic displacement parameter is nearly twice as high, U = 0.126 $Å^2$, as those of the other well-known H positions. Model **C** in the current report has a similar result, not significantly different from

that of Parimita et al. (2007). Calculation of an electron density difference map prior to including this proton showed an extension of electron density in the enolizable proton region extending between the two O atoms with a slight preponderance of electron density nearer to O3. A similar electron density difference pattern is seen in the room temperature X-ray diffraction study of the closely related tetrahydocurcumin structure (Girija, Begum, Syed, & Thiruvenkatam, 2004) which was successfully modeled as a nonstatistical disorder of the two enol H positions.

Several models were explored for the disordered enol positions. A statistical disorder (two half H atoms) with idealized O—H distances (similar to Girija et al., 2004) and a single refined isotropic atomic displacement parameter gave a reasonable result with U[H3O] = U[H4O] = 0.068 Å^2, a value at the upper end of the range of those of other well-known H atom positions in the same structure. Relaxing the enol O—H distance restraint brought the shared isotropic U down to 0.057 Å^2, well in the range of other well-known H-atom positions. On removing the constraint of equal U values for the two enol H-atom positions, the one nearer O3 became smaller (indicating a higher occupancy) and the one nearer O4 became larger (indicating a lower occupancy). The final model restrained the O3–H3O and O4–H4O distances to be similar, refined the common U value, and refined an occupancy factor for H3O and H4O, resulting with a slightly higher occupancy for H3O. This final model, illustrated in Figure 3, is in close agreement with the nonstatistical disorder model of Girija et al. (2004) and the energy values and proton probability distribution reported by Kong et al. (2014).

A summary of the previously reported crystalline polymorphs is presented in Table 2. The crystal structure in this work is included in Table 2 as column IV. The structure in this study is in the monoclinic space group P2/n, the same as that of polymorph I. The solubility of cocrystals of curcumin have recently been studied using supercritical fluid technology (Ribas et al., 2019) and are reported to have higher dissolution rates than pure curcumin in water medium.

Table 2 Crystal data and polymorphs

Crystal data	I	II	III	IV
Space group	$P2/n$	$Pca2_1$	$Pbca$	$P2/n$
Temperature (K)	100	100	100	298
a, (Å)	12.5676(11)	35.417(3)	12.536(3)	12.6956(3)
c	7.0425(6)	7.7792(7)	7.9916(17)	7.2093(2)
b	19.9582(18)	12.6482(11)	34.462(7)	19.9362(5)
α, (°)	90	90	90	90
β	94.987(1)	90	90	95.276(2)
γ	90	90	90	90
V (Å^3)	1759.8(3)	3484.7(5)	3452.3(13)	1816.96(8)
D_{calcd}/g cm^{-3}	1.390	1.404	1.417	1.347
Z/Z′	4/1	8/2	8/1	4/1
$R_1[I > 2\sigma(I)]$	0.0435	0.0513	0.0893	0.0512
wR_2 (all)	0.1163	0.1218	0.1681	0.1575
Goodness-of-fit (S)	1.054	1.083	0.930	1.087

Analysis of the hydrogen bonding shows the presence of O–H···O intramolecular hydrogen bond interactions in the structure as summarized in Table 3. A strong hydrogen bond forms in the enol ring as shown in Figure 5. The intramolecular O⋯O distance of the O1–H1⋯O2 interaction forming the ring is 2.684(2) Å, in the lower end of the O–H···O hydrogen bond distances range of 2.470(2) to 3.028(2)Å, with an angle of 113.4° indicating a strong hydrogen bond. The formation of the strong intramolecular interaction in the enol ring leads to electron delocalization between –CO–CH=COH fragment and indicated the strong hydrogen bond (Matlinska et al., 2018; Arrieta, Haglund, & Mostad, 2000; Mostad, 1994) and this may be characterized as the third ring in the molecule. Intermolecular interactions are linked by O1–H1···O4 [x-0.5, y-1, z+0.5] and O6–H6···O3 [x+1, y, z] with O⋯O hydrogen bond distances of 2.841(2) and 3.028(2), respectively.

Table 3 Selected hydrogen bond interaction parameters (A˚, °)

D–H···A	*D*–H	H···*A*	*D*···*A*	D–H···*A*
O1–H1···O2	0.82	2.25	2.684(2)	113.7
O1–H1···O4	0.82	2.11	2.841(2)	149.2 [x-0.5, y-1, z+0.5]
O3–H3O···O4	0.76(3)	1.76(3)	2.4696(19)	156(4)
O4–H4O···O3	0.76(3)	1.75(3)	2.4696(19)	159(5)
O6–H6···O3	0.82	2.61	3.028(2)	113.4 [x+1, y, z]

Symmetry code i) x, y, z; ii) x+1, y, z; iii) x-0.5, y-1, z+0.5

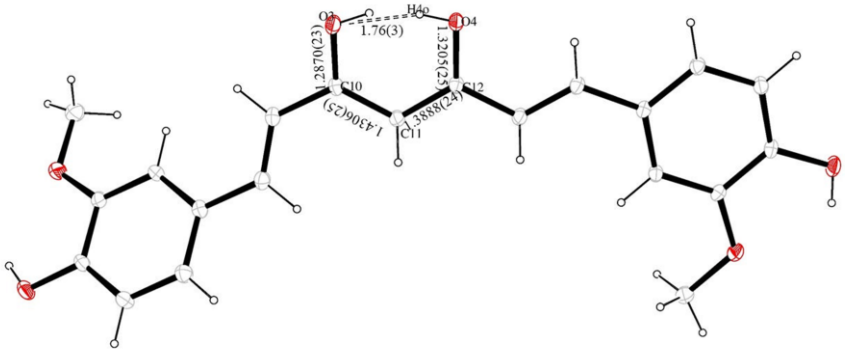

Figure 5 Hydrogen bond formation and geometry of the enol ring

Weak intermolecular hydrogen bonds support the overall packing of the curcumin molecules (Figure 6). The bifurcated C–H···O bonds link through the phenoxy O–H acceptor with the distance of 4.046(3) Å is characteristic of a weak hydrogen bond. Weak C–H···O hydrogen bonds in curcumin crystal structure have been reported by Sanphui et al. (2011). Graph set notation (Bernstein, Davis, Shimoni, & Chang, 1995; Etter, MacDonald, & Bernstein, 1990) in the crystal is assigned as the R_6^2 (36) pattern (Figure 7). The variety of hydrogen bonds generate the different packing motifs which may alter the molecular conformations. This may have a significant impact on the solubility and bioavailability of curcumin (Girija et al., 2004).

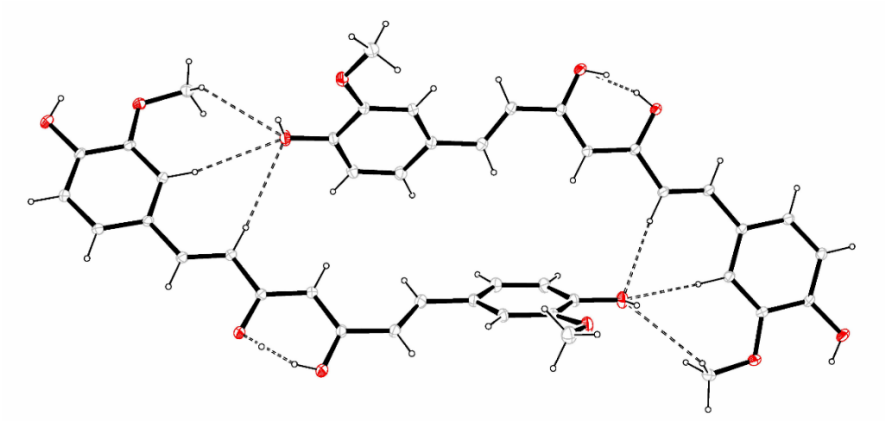

Figure 6 Graph set notation of the curcumin molecule

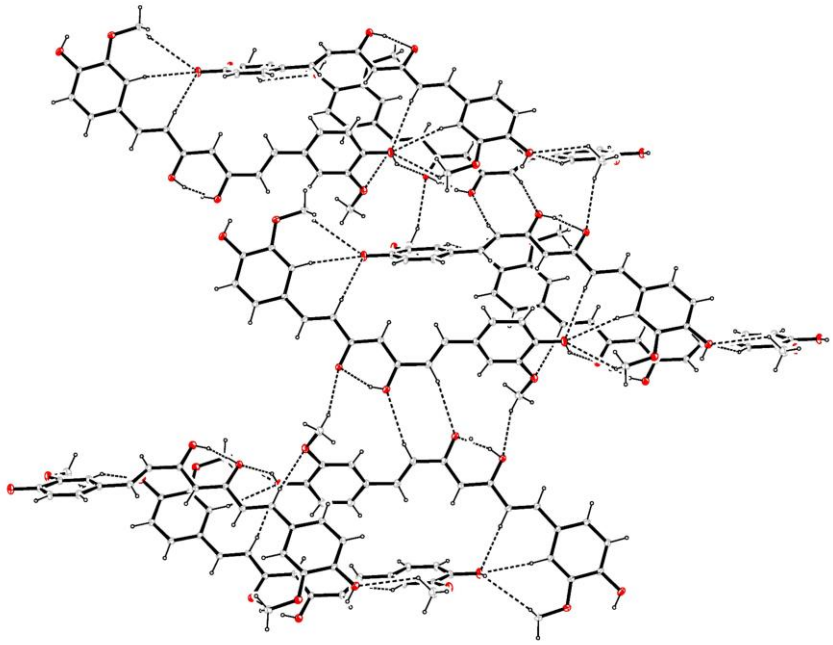

Figure 7 A packing diagram for curcumin showing a hydrogen bonded sheet of the molecule *via* O–H···O and C–H···O interactions

The intermolecular interactions of the title compound are quantified using Hirshfeld surface analysis. Hirshfeld surface analysis is a useful tool to analyze the most dominant intermolecular interactions in the crystal structure (Spackman & Jayatilaka, 2009). Figure 8 shows all close contacts in the molecule as red spots over the surface indicating the intermolecular contacts involved in the hydrogen bonds which are connected by O1–H1···O4, C1–H1a···O4, and C14–H14···O2, respectively.

JCST Vol. 9 No. 2 Jul.-Dec. 2019, pp. 77-87
ISSN 2630-0583 (Print)/ISSN 2630-0656 (Online)

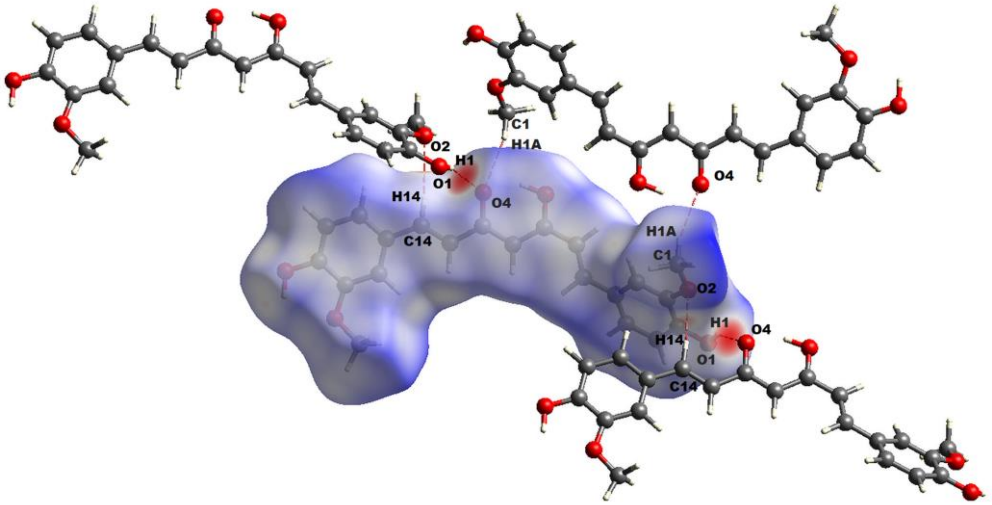

Figure 8 Hirshfeld surface analysis of curcumin crystal structure

In addition, the interactions in the fingerprint plot are represented as blue spikes. The distance d_i represents the distance from the surface to the nearest atom interior to the surface, and the distance d_e represents the distance from the surface to the nearest atom exterior to the surface (Spackman & Jayatilaka, 2009). The combination of d_i and d_e in the form of two-dimensional fingerprint plots gives a summary of close contacts in the crystal lattice. Figure 9 displays the close contacts for H···H, C–H, and H···O interactions are found at 41.1, 25.6 and 25.2 percent, respectively. In this study the fingerprint plots indicated that the interactions in the molecular packing of curcumin are longer contact distances which are in agreement with Desiraju (2005) that the aromatic hydroxyl does not form a good C–H···O contact (Sarma & Desiraju, 1987). The crystal molecular packing of curcumin is linked by the weak interactions. The packing of the curcumin molecules may be further stabilized by the network of H···H interaction.

.

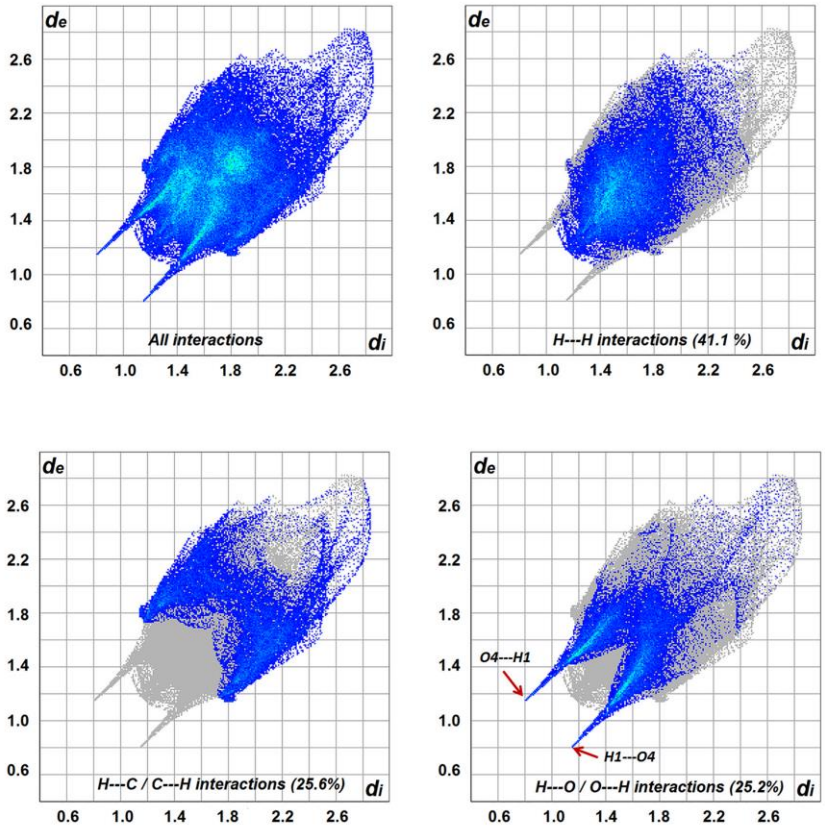

Figure 9 Fingerprint plot from Hirshfeld surface analysis of the hydrogen bonding in the asymmetric unit

5. Conclusion

A major problem of curcumin for use as a bioactive herbal therapeutic agent and/or functional food is its low solubility and low bioavailability. This study is providing information of curcumin structure to the understanding of the interactions in the crystal structure. These observations could aid in modifying the curcumin structure to form faster dissolving solid cocrystal forms with very soluble and relatively stable conformers useful for drug development in the future.

6. Supporting information

CCDC 1957790 contains the supplementary crystallographic data for this paper. The data can be obtained free of charge from The Cambridge Crystallographic Data Centre via www.ccdc. cam.ac.uk/structures.

7. Acknowledgements

This study was supported by the Research and Development Institute, Nakhon Ratchasima Rajabhat University.

8. References

Arrieta, A. F., Haglund, K. A., & Mostad, A. (2000). Conjugation and hydrogen bonding in a curcumin analogue. *Acta Crystallography Section C, 56*(Pt 12), e594-e595. DOI: 10.1107/S0108270100015729

Bernstein, J., Davis, R. E., Shimoni, L., & Chang, N.-L. (1995). Patterns in hydrogen bonding: Functionality and graph set analysis. *Angewandte Chemie International Edition England*, *34*(15), 1555-1573. DOI: 10.1002/anie.199515551

Chavda, H. V., Patel, C. N., & Anand, I. S. (2010). Biopharmaceutics Classification System. *Systematic Reviews in Pharmacy, 1*(1), 62-69. DOI: 10.4103/0975-8453.59514

Desiraju, G. R. (2005). C–H···O and other weak hydrogen bonds. From crystal engineering to virtual screening. *Chemistry Communication*, *28*(24), 2995-3001. DOI: 10.1039/B504372G

Desiraju, G. R. (2018). Crystal engineer, crystals and crystallography. *IUCrJ, 5(Pt 6)*, 660-660. DOI: 10.1107/S2052252518015014

Dolomanov, O. V., Bourhis, L. J., Gildea, R. J, Howard, J. A. K., & Puschmann, H. (2009). *OLEX2*: a complete structure solution, refinement and analysis program. *Journal of Applied Crystallography*, *42*(2), 339-341. DOI: 10.1107/S0021889808042726

Etter, M., MacDonald, J. C., & Bernstein, J. (1990). Graph-set analysis of hydrogen-bond patterns in organic crystals. *Acta Crystallography section B*, *46*(Pt 2), 256-262. DOI: 10.1107/S0108768189012929

Farrugia, L. J. (2012). *WinGX* and *ORTEP* for Windows: an update. *Journal of Applied Crystallography*, *45*(4), 849-854. DOI: 10.1107/S0021889812029111

Girija, C. R., Begum, N. S., Syed, A. A. & Thiruvenkatam, V. (2004). Hydrogen-bonding and C—H···π interactions in 1,7-bis(4-hydroxy-3-methoxyphenyl)heptane-3,5-dione (tetrahydrocurcumin). *Acta Crystallographica Section C, 60*(Pt 8), o611-o613. DOI: 10.1107/S0108270104015549

Hubschle, C. B., Sheldrick, G. M., & Dittrich, B. (2011). *ShelXle*: a Qt graphical user interface for *SHELXL*. *Journal of Applied Crystallography*, *44*, 1281-1284. DOI: 10.1107/S0021889811043202.

Hutchins, K. M. (2018). Functional materials based on molecules with hydrogen-bonding ability: applications to drug co-crystals and polymer complexes. *Royal Society Open Science*, *5*(6), 180564. http://dx.doi.org/10.1098/rsos.180564

Ishigami,Y., Goto, M., Masuda, T., & Suzuki, S. (1999). The crystal structure and the fluorescent properties of curcumin. *Journal of the Japan Society of Colour Materials*, *72*(2), 71-77.

Jeffrey, G. A., & Saenger, W. (1991). *Hydrogen Bonding in Biological Structures*. New York, USA: Springer.

Kong, X., Brinkmann, A., Terskikh, V., Wasylishen, R. E., Bernard, G. M., Duan, Z., . . . Wu, G. (2014). Proton probability distribution in the O···H···O low-barrier hydrogen bond: A combined solid-state NMR and quantum chemical computational study of dibenzoylmethane and curcumin. *Journal of Physical Chemistry B*, *120*(45), 11692-11704. DOI: 10.1021/acs.jpcb.6b08091

Matlinska, M. A., Wasylishen, R. E., Bernard, G. M., Terskikh, V. V., Brinkmann, A., & Michaelis, V. K. (2018). Capturing elusive polymorphs of curcumin: A structural characterization and computational study. *Crystal Growth and Design*, *18*(9), 5556-5563. DOI: 10.1021/acs.cgd.8b00859

Mostad, A. (1994). Structure studies of curcuminoids. VIII. Crystal and molecular structure of 4-benyl-1,7-diphenyl-1,6-heptadiene-3,5-dione. *Acta Chemica Scandinavica*, *48*, 144-148. DOI: 10.3891/acta.chem.scand.48-0144

Nangia, A. K., & Desiraju, G. R. (2018). Crystal Engineering. An Outlook for the Future. *Angewandte Chemie International Edition*, *58*(13), 4100-4107. DOI: 10.1002/anie.201811313

Parimita, S. P., Ramshankar, Y. V., Suresh, S., & Guru Row, T. N. (2007). Redetermination of curcumin: (1*E*,4*Z*,6*E*)-5-hydroxy-1,7-bis(4-hydroxy-3-methoxyphenyl)hepta-1,4,6-trien-3-one. *Acta Crystallographica*

Section C, *63*(2), o860-o863. DOI: 10.1107/S160053680700222X

Ribas, M. M., Sakata, G. S. B., Santos, A. E., Magro, C. D., Aguiar, G.-P S., Lanza, M., & Oliveira, J. V. (2019). Curcumin cocrystals using supercritical fluid technology. *The Journal of supercritical fluids*, *152*, 104564. DOI: 10.1016/j.supflu.2019.104564

Sanphui, P., Goud, N. R., Khandavilli, R. U. B., Bhanoth, S., & Nangia, A. (2011). New polymorphs of curcumin. *Chemistry Communication*, *47*, 5013-5015. DOI: 10.1039/C1CC10204D

Sanphui, P., Goud, N. R., Khandavilli, R. U. B., & Nangia, A. (2011). Fast Dissolving Curcumin Cocrystals. *Crystal Growth and Design*, *11*(9), 4135-4145. DOI: 10.1021/cg200704s

Sarma, J. A. R. P., & Desiraju, G. R. (1987). C–H···O interactions and the adoption of 4 Å short-axis crystal structures by oxygenated aromatic compounds. *Journal of Chemical Society Perkin Transaction 2*, 1195-1202. DOI: 10.1039/P29870001195

Sathisaran, I., & Dalvi, S. V. (2017). Crystal engineering of curcumin with salicylic acid and hydroxyquinol as coformers. Crystal Growth and Design, 17(7), 3974-3988. https://doi.org/10.1021/acs.cgd.7b00599

Sheldrick, G. M. (2015a). *SHELXT*–Integrated space-group and crystal structure determination. *Acta Crystallographica Section A*, *71*, 3-8. DOI: 10.1107/S2053273314026370

Sheldrick, G. M. (2015b). Crystal structure refinement with *SHELXL*. *Acta Crystallographica Section C*, *71*, 3-8. DOI: 10.1107/S2053229614024218

Skieneh, J. M., Sathisaran, I., Dalvi, S. V., & Rohani, S. (2017). Co-amorphous form of curcumin-folic acid dehydrate with increased dissolution rate. *Crystal Growth and Design*, *17*, 6273-6280. DOI: 10.1021/acs.cgd.7b00947

Spackman, M. A., & Jayatilaka, D. (2009). Hirshfeld surface analysis. *Crystal Engineering Communication*, *11*, 19-32. DOI: 10.1039/B818330A

Tonnessen, H. H., Karlsen, J., & Mostad, A. (1982). Structural studies of curcuminoids. I. The crystal structure of curcumin. *Acta Chemica Scaninavica B, 36b*, 475-479. DOI: 10.3891/acta.chem.scand.36b-0475